High Resolution Wide Swath SAR Imaging with Digital Beamforming – Performance Analysis, Optimization, System Design

Nicolas Gebert, DLR, Germany
Gerhard Krieger, DLR, Germany
Alberto Moreira, DLR, Germany

Abstract

Multi-aperture synthetic aperture radar (SAR) systems in combination with an appropriate coherent processing of the individual aperture signals enable high resolution wide swath (HRWS) SAR imaging [1]-[8]. An innovative reconstruction algorithm for such a digital beamforming on receive was presented in [9]-[12] that allows for HRWS even in case of a non-uniformly sampled data array in azimuth. This paper will compare this algorithm to different azimuth processing strategies regarding their performance in dependency of the overall sampling. Further, the algorithm is characterized theoretically regarding aliasing and residual ambiguities. In this context, optimization strategies are discussed to maximize the system's performance by pattern tapering on transmit and "Pre-Beamshaping on Receive" networks that adaptively adjust the virtual sample positions.

1 Introduction

1.1 Multi-Aperture Sampling

Several innovative techniques using multiple receive apertures ('Rx') have been suggested to overcome the inherent limitations of conventional SAR to perform HRWS imaging [1]-[8]. For optimum performance the relation between sensor velocity v and the along-track offsets Δx of the N sub-apertures has to result in equally spaced effective phase centers thus leading to a uniform sampling of the received signal (cf. Fig. 1, left). This requires the following relation:

$$PRF_{opt} = \frac{2 \cdot v}{N \cdot \Delta x} \tag{1}$$

If a non-optimum PRF is chosen, the gathered samples are spaced non-uniformly. This requires a further processing step after down-conversion and quantization of the multi-aperture azimuth signal before conventional monostatic focusing algorithms can be applied. For this, the individual aperture signals are regarded as independent Rx channels (cf. Fig. 1, right). The purpose of the azimuth processing is to combine the N channels, each of bandwidth $N \cdot PRF$ but sub-sampled with PRF, to obtain a signal effectively sampled with $N \cdot PRF = PRF_{eff}$. Thus the Nyquist criterion is fulfilled in average after the processing, which yields - in the optimum case - an output signal that is free of aliasing.

2 Azimuth Processing

2.1 Algorithms

In the following, three more methods to process the azimuth signal of a multi-aperture signal are presented and compared to the „reconstruction algorithm".

1) Displaced Phase Center Antenna (DPCA): This technique proposes to recover the azimuth signal by interleaving the samples of the different Rx channels without any further processing [1]. Consequently, the stringent timing requirement of Eq. (1) has to be fulfilled to obtain a signal that is equivalent to a monostatic signal of N times the PRF. In any other case the sample positions deviate from the ideal positions, but they are treated as if the signal was sampled uniformly.

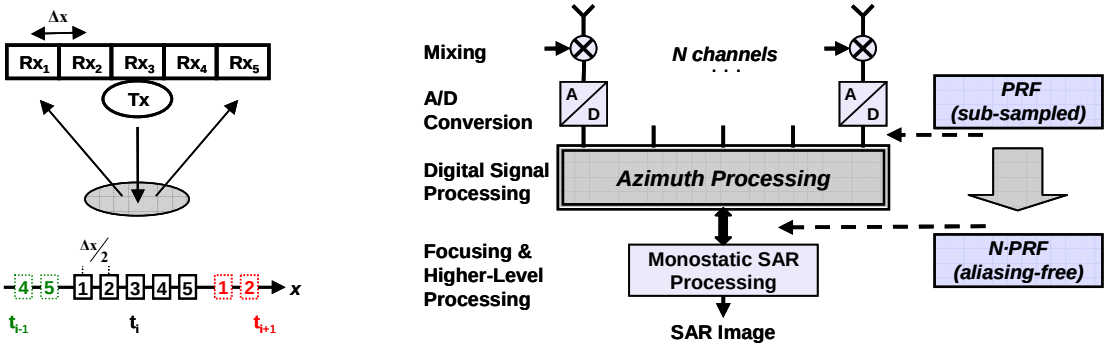

Fig. 1: **Left**: **Multi-Aperture System** consisting of 5 Rx apertures and a separate Tx antenna and corresponding **virtual sample positions** for subsequent pulses t_{i-1}, t_i, t_{i+1}. **Right**: **Block diagram of the processing**. After down-converting and digitizing every aperture's signal, the azimuth processing combines N aliased channels to one output signal with N times the original sampling ratio.

2) Phase Correction: This method takes the properties of the SAR signal into account. It is based on an analysis of the multi-aperture signal's phase compared to the phase of a monostatic and uniformly sampled signal. This yields a phase difference depending on Doppler frequency. By applying an appropriate phase correction to the multi-aperture data, its phase is adjusted in a way such that the resulting phase corresponds to the monostatic and uniformly sampled signal. [3]

3) The **Reconstruction Algorithm** is based on solving a system of linear equations to unambiguously recover the formerly aliased azimuth spectrum. A detailed derivation and investigation can be found in [9]-[12]. As already indicated in [9], this method comprises the approach in 4) and leads to nearly identical results in a single platform system.

4) Null-Steering: This space-time approach is based on adaptively adjusting the weighting coefficients of the azimuth channels to steer the nulls in the resulting joint antenna pattern to the angles corresponding to the ambiguous Doppler frequencies. This corresponds to a spatial filtering of the data to suppress ambiguous frequencies in the azimuth signal. [13]

2.2 Reference System

Fig. 1, left and Table I summarize the main parameters of the investigated HRWS SAR system. The Rx antenna pattern was approximated by a *sin(x)/x* pattern while a Bessel-function was used for the Tx antenna.

Parameter	Symbol	Value
Carrier wavelength	λ	3.1 cm
Orbit height	h_{sat}	530 km
Swath-width	L_{sw}	80 km
Mean incident angle	Θ_i	40.5°
Rx Sub-apertures in azimuth	N	5
Rx Sub-aperture length in azimuth	$d_{a,rx}$	3.2 m
Tx Dish antenna in azimuth	$d_{a,tx}$	3.5 m
Sensor velocity	v	7600 m/s
Processed azimuth bandwidth	B_{Dop}	5.064 Hz

TABLE I. Main parameters of the investigated SAR system.

2.3 Performance

The performance analysis is done by simulating the point target response resulting from the different processing methods. It is performed for a varying *PRF* of 1 kHz to 2 kHz what corresponds to varying sampling scenarios of the system.

2.3.1 Azimuth Ambiguity Suppression

The ambiguous energy suppression represents the logarithmic ratio of the integrated energy of the first 10 ambiguities to the 'real' target's energy of the impulse response. For 1188 Hz and 1583 Hz samples of different sub-apertures coincide spatially causing the processing to fail what results in the peaks. A simple solution to this problem could be to combine the RF signals of the respective coinciding channels yielding a more suitable sampling scheme for the processing. (See also 4.2.)

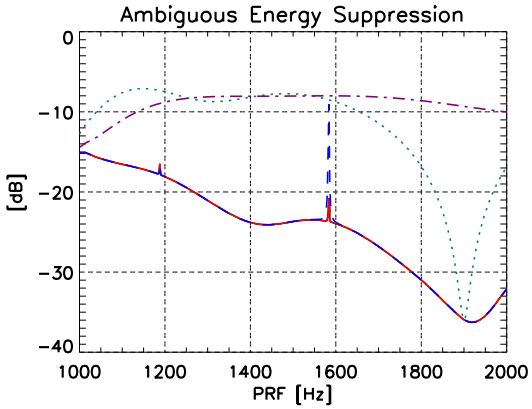

Fig. 2. Ambiguity suppression vs. *PRF*. Phase Correction (Dotted green) and DPCA (dotted-dashed violet) show significantly worse suppression than Reconstruction (red) and Null-Steering (dashed blue) that are nearly identical.

2.3.2 Resolution

The resolution gives the 3-dB width of squared amplitude of the impulse response's mainlobe.

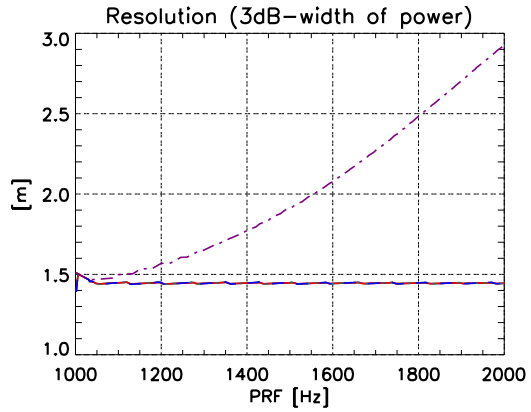

Fig. 3. Resolution vs. *PRF*. Phase-Correction (Dotted green), Reconstruction (red) and Null-Steering (dashed blue) provide a constant resolution of 1.45 m while it degrades for DPCA (dotted-dashed violet) for increasing *PRF*.

2.3.3 SNR / Scaling of Noise Power

As presented in [11], the azimuth processing with the reconstruction algorithm may cause a rise of the noise floor that increases with increasing non-uniformity of the sampling showing singular values for the critical *PRFs* mentioned in 2.3.1 (cf. Fig. 4). The same inconveniences occur for the null-steering approach while in the case of the Phase Correction processing the noise floor remains constant. Regarding the DPCA approach,

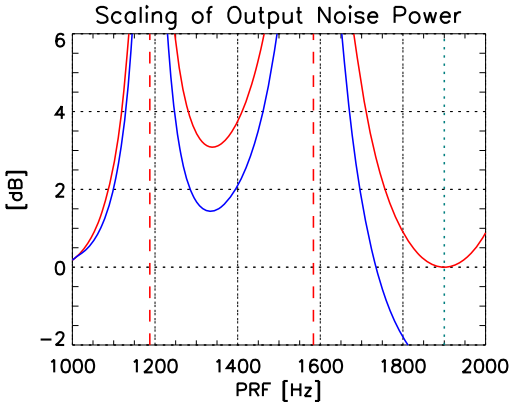

Fig. 4. Scaling of Noise Power vs. *PRF* before focusing (red) and afterwards (blue) considering the gain due to over-sampling.

the noise power is not increased but a significant loss of peak power of the focused target can be observed for increasing non-uniform sampling.

2.3.4 Summary Azimuth Processing

We have seen that more the sophisticated approaches like null-steering and reconstruction algorithm provide efficient ambiguity suppression and constant resolution over a varying *PRF*, while the other methods fail. But as indicated in 2.3.3, a possible rise of noise power depending on the overall sampling has to be considered.

2.4 Adaptation of Sensor Dimensions

In a next step, the system presented in 2.2 is modified to obtain improved ambiguity suppression and mitigate the inconveniences arising from the scaling of the noise power. The modification comprises a Rx aperture that is shortened to 2.8 from 3.2 m and the enlargement of the Tx-dish from 3.5 to 5 m. The new overall Rx antenna length of 14 m yields an optimum *PRF* of 1085 Hz that is adapted to the timing[1] what limits the maximum scaling of the output noise in the considered interval[1] to 2 dB before and 1 dB after focusing. In addition to that, the increased dish size results in distinct improved ambiguity suppression over a wide *PRF*-range (cf. Fig. 5) at the expense of a slight increase of resolution from 1.45 to 1.55 m in the modified system.

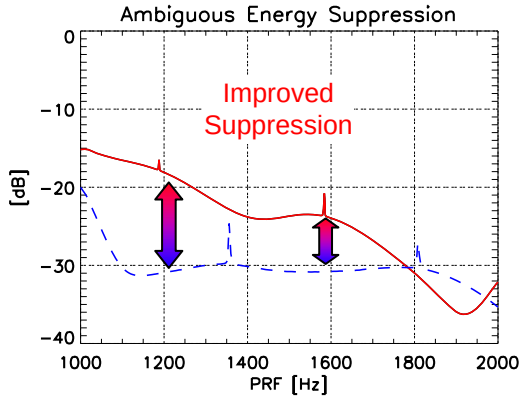

Fig. 5. Ambiguity suppression vs. *PRF*. Improved suppression of the modified system (dashed blue) compared to the original system (solid red) over a wide range of *PRF*.

3 Residual Ambiguity Estimation

In [11] and [12] it was demonstrated that aliasing disturbs the unambiguous reconstruction of the multi-aperture SAR signal. This is due to the fact, that only the aliased energy within the band *[-N·PRF/2, N·PRF/2]* of the original signal is cancelled by the reconstruction. All energy outside this band - but after sampling with *PRF* inside the considered bandwidth of the discrete signal - is not well suppressed and finally gives rise to ambiguities in the reconstructed signal. With knowledge of the overall configuration and the antenna patterns, the spectral "error" that remains from the aliased signal after reconstruction can be derived. The error represents the remaining ambiguous signal and can be expressed as a sum of errors E_k that cause the ambiguity of order k w.r.t. *PRF*. E_k is made up of contributions from each receiver j that are expressed by the monostatic SAR signal $U(f)$ multiplied by the respective $H_j(f)$. Further, the processing of the signal is expressed by the filters P_{ij}, that are defined on N sub-bands I_i, each of length *PRF* and situated within *[-(N/2+i-1) ·PRF, -(N/2+i)·PRF]*. The restriction on I_i is done by the rectangular window function $\Pi(f/I_i)$.

$$E_k = \sum_{i=1}^{N}\sum_{j=1}^{N} \underbrace{U_k(f)\cdot H_{jk}(f)}_{\#1} \cdot \underbrace{\Pi\left(f/I_i\right)\cdot P_{ji}(f)}_{\#2} \qquad (2)$$

$$U_k(f) = U(f + k\cdot prf)\ ;\ H_{jk}(f) = H_j(f + k\cdot prf) \qquad (3)$$

The index k indicates a shift by k times the *PRF* due to the sub-sampling. This means that the *k-th* continuation of the original spectrum gives rise to the ambiguity of order k. Hence contribution #1 in Eq. (2) gives the spectral appearance of the *k-th* continuation of the signal as seen by Rx j, while #2 represents the processing applied to this signal in the respective sub-band I_i. This can be rearranged to an expression describing the spectral properties of the signal by U_{ki} and the influence of the system's configuration by W_{jki}:

$$E_k = \sum_{i=1}^{N}\sum_{j=1}^{N} \underbrace{U_k(f)\cdot\Pi\left(f/I_i\right)}_{:=U_{ki}} \cdot \underbrace{H_{jk}(f)\cdot P_{ji}(f)}_{:=W_{jki}} \qquad (4)$$

Assuming a normalized matched filter for focusing and applying the principle of stationary phase, we obtain S_k giving the ambiguous part of order *'k'* of the system's impulse response in dependency of the antenna pattern A, the Doppler modulation coefficient β and a phase term φ_c accounting for the remaining phase difference after focusing due to the non-linear characteristic of the Doppler-frequency f. The azimuth spectrum is restricted to the processed Bandwidth B_P by $\Pi(f/B_P)$.

$$S_k(f) = A\left(\frac{f + k\cdot prf}{\beta}\right)\cdot e^{j\varphi_c}\cdot\Pi\left(\frac{f}{B_P}\right)\cdot\sum_{i=1}^{N}\Pi\left(\frac{f}{I_i}\right)\cdot W_{k,i} \qquad (5)$$

Finally, applying an inverse Fourier transform to S_k allows for estimating the residual ambiguities.

4 Optimized System Concepts

4.1 Pattern Tapering on Transmit

As derived in 3, all spectral signal energy outside the band *[-N·PRF/2, N·PRF/2]* gives rise to ambiguities. This can be avoided by confining the Doppler bandwidth of the signal to *N·PRF* by an appropriate antenna pattern. As enlarging the Tx antenna can achieve this only at the expense of resolution (cf. 2.4), an adapted tapering can provide an improved ambiguity suppression without degrading resolution. To demonstrate the potential of tapering, we consider the system of 2.4 and investigate different combinations of Tx antennas and excitations (cf. Table II) that can be either realized by a separate Tx antenna or by using an active array that offers the flexibility to use parts of the Rx antenna for transmit. The scenarios show a resolution (B_P = 4.1 kHz) equivalent to the dish antenna system and are compared to the "classical" system, where the Tx and

[1] An analysis of the timing diagram of the system yields a necessary *PRF* range from 1.1 to 1.25 kHz to cover completely the incident angle range from 20-50° with a swath-width of 80 km.

Length	Excitation	Pattern	Resolution
5 m (dish)	uniform	Bessel	1.75 m
14 m	*sin(x)/x*	Rectangular	1.75 m
6.2 m	triangular	$(sin(f_x)/f_x)^2$	1.75 m
2.8 m	uniform	$sin(f_x)/f_x$	1.65 m

TABLE II. Excitations and corresponding antenna patterns.

Rx aperture have the same size what results in a slightly improved resolution of 1.65 m. The resulting ambiguity suppression in Fig. 6 is worst for the uniform excitation and is already improved by more than 10 dB using a 6.2 m antenna with a simple triangular tapering and finally results in the quasi-optimum - as it approximates a rectangular pattern - *sin(x)/x* excitation. The plot is completed by the curve of the separate dish antenna, that runs similarly to the $(sin(f_x)/f_x)^2$ pattern but with less variation vs. *PRF*. Especially the unconventional *sin(x)/x*-excitation demonstrates the potential of tapering to efficiently cancel the spurious spectral components while preserving the resolution. A full exploitation of the benefits of tapering requires a fine adjustment of antenna dimensions, *PRF* and B_P, taking into account the trade-off between resolution and ambiguity suppression.

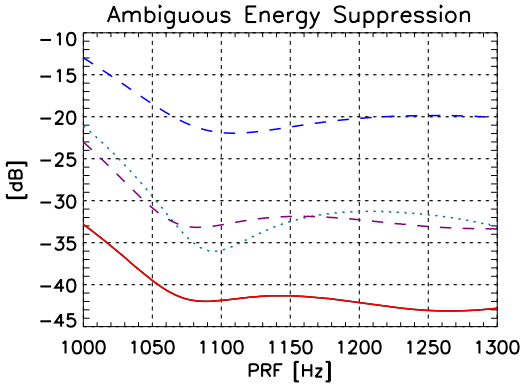

Fig. 6. Ambiguous Energy Suppression with pattern tapering: The "rectangular" pattern (solid red), a separate Tx dish (dashed violet), the triangular (dotted green) and the uniform excitation (dashed blue). The *PRF* range from 1 to 1.3 kHz covers the relevant interval from 1100 to 1250 Hz with respect to the timing.

4.2 Pre-Beamshaping on Receive

Pre-Beamshaping on Receive is a technique based on an antenna consisting of a large number of individual apertures. These apertures are followed by a network that allows for an individual and reconfigurable combination of the -already amplified- apertures' RF signals. Then A/D conversion is performed yielding a number of adapted "channels" with optimized properties (cf. Fig. 7). This offers the opportunity for flexibly adjusting the virtual sample positions to adapt the sampling scenario to the actual configuration. In addition to that, such networks enable pattern tapering on Rx what offers a powerful tool to e.g. suppress ambiguities and optimize the system. Further, the RF signal of each aperture can be used for multiple combinations hence exploiting optimally the signal energy.

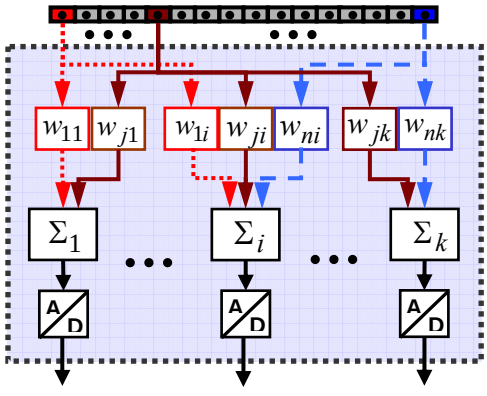

Fig. 7. "Pre-Beamshaping on Receive" network. Amplified RF signals of various apertures are adaptively weighted and combined before A/D conversion yields the optimized output channels.

4.3 Adaptive *PRF* Management

Finally, an adaptive management of the *PRF* to adjust the virtual sample positions can be used to minimize the non-uniformity of the overall sampling. This approach is especially of interest in sparse arrays, as the spatial position of adjacent samples is not bound to the transmitted pulse as in single platform systems. This offers wide flexibility to adapt the sampling.

5 Discussion

A comparison of azimuth processing methods for multi-aperture signals showed that only the reconstruction algorithm and the null-steering approach provide high resolution in combination with efficient ambiguity suppression. For these approaches, a modified system with improved ambiguity suppression was presented and a mathematical expression estimating the residual ambiguities was derived. Further, optimization strategies were investigated showing the potential of pattern tapering on Tx to improve the ambiguity suppression while preserving the resolution. Finally, pre-beamshaping on receive networks were proposed, offering various optimization potentials by adapting the system's virtual sampling and performing tapering on Rx.

References

[1] G.D. Callaghan and I.D. Longstaff, *Wide Swath Spaceborne SAR Using a Quad Element Array*, IEE Radar Sonar and Navigation 146(3), pp 159-165, 1999

[2] M. Suess, B. Grafmüller, R. Zahn, *A Novel High Resolution, Wide Swath SAR System*, IGARSS 2001

[3] M. Younis, C. Fischer, W. Wiesbeck, *Digital Beamforming in SAR systems*, IEEE Trans. Geosci. Remote Sensing 41 (7), 2003

[4] L. Brule, H. Baeggli, *Radarsat-2 Program Update*, IGARSS 2002.

[5] J. Mittermayer, H. Runge, *Conceptual Studies for Exploiting the TerraSAR-X Dual Receiving Antenna*, IGARSS 2003.

[6] N.A. Goodman, S.C. Lin, D. Rajakrishna, J.M. Stiles, *Processing of Multiple-Receiver Spaceborne Arrays for Wide Area SAR*, IEEE Trans. Geoscience and Remote Sensing 40 (4), pp 841-852, 2002

[7] G. Krieger and A. Moreira, *Potentials of Digital Beamforming in Bi- and Multistatic SAR*, IGARSS 2003

[8] J.P. Aguttes, *The SAR Train Concept: Required Antenna Area Distributed over N Smaller Satellites, Increase of ...* , IGARSS 2003

[9] G. Krieger, N. Gebert, A. Moreira, *Unambiguous SAR Signal Reconstruction from Non-Uniform Displaced Phase Centre Sampling*, IEEE Geoscience and Remote Sensing Letters, Vol. 1, No. 4, October 2004

[10] G. Krieger, N. Gebert, A. Moreira, *Unambiguous SAR Signal Reconstruction from Non-Uniform Displaced Phase Centre Sampling*, IGARSS 2004

[11] N. Gebert, G. Krieger, A. Moreira, *SAR Signal Reconstruction from Non-Uniform Displaced Phase Centre Sampling in the Presence of Perturbations*, IGARSS 2005

[12] N. Gebert, G. Krieger, A. Moreira, *High Resolution Wide Swath SAR Imaging – System Performance and Influence of Perturbations*, IRS'05

[13] H. Li, H. Wang, T. Su, Z. Bao, *Generation of Wide-Swath and High-Resolution SAR Images From Multichannel Small Spaceborne SAR System*, IEEE Geoscience and Remote Sensing Letters, Vol. 2, No. 1, Jan. 05